ELSEVIER

Physica C 317–318 (1999) 142–148

PHYSICA C

On anomalous temperature dependence of $H_{C2\perp}$ in natural and artificial layer superconductors

M. Ikebe [a,*], H. Fujishiro [a], Y. Obi [b], H. Fujimori [b], S. Morohashi [c]

[a] *Department of Materials Science, Faculty of Engineering, Iwate University, 4-3-5 Ueda, Morioka 020-8551, Japan*
[b] *Institute for Materials Research, Tohoku University, 2-1-1 Katahira, Sendai 980-8577, Japan*
[c] *Faculty of Engineering, Yamaguchi University, 2557 Tokiwadai, Ube 755-8611, Japan*

Abstract

Anomalous temperature dependence of the perpendicular critical field $H_{C2\perp}(T)$ of layered transition metal dichalcogenide MX_2 with and without pyridine intercalation and that of Nb/Al_2O_3 superlattice are consistent with the theory of Maekawa, Ebisawa and Fukuyama (MEF) [S. Maekawa, H. Ebisawa, H. Fukuyama, J. Phys. Soc. Jpn. 52 (1983) 1352] based on the weak Anderson localization. For the pure conductor 2H-$NbSe_2$, however, the anomalous $H_{C2\perp}(T)$ is to originate from the anisotropies in the Fermi surface and energy gap through the effect of nonlocality.

Keywords: $H_{C2\perp}$; Artificial layer superconductor; Natural layer superconductor

1. Introduction

Superconductors with layered structures have long been model systems to investigate anisotropic and two-dimensional (2D) properties of superconductivity. Historically, the transition metal dichalcogenides MX_2 (M = Nb, Ta: X = S, Se, etc.) [1] were firstly and most extensively studied among the various layer-metal systems because they are rich in physical properties, having various polytypes of the crystal structure. Another attractive point of MX_2 is their ability to accept various organic molecules as an intercalant between layers. As a result of intercalation, the anisotropy is generally markedly increased, and quasi-2D superconductivity was first established in this system [2–5]. The most characteristic feature of quasi-2D superconductivity is the phenomenon of the dimensional crossover, which causes a clear upturn at the crossover temperature T_D in the temperature dependence of the parallel critical field ($H_{C2\parallel}$).

With recent progress in the film deposition techniques, on the other hand, superconductivity of artificial multilayers has also been widely investigated and the dimensional crossover phenomenon in $H_{C2\parallel}(T)$ associated with quasi-2D superconductivity has been reported for superconductor/insulator (S/I) [6,7], superconductor/normal–metal (S/N) [8,9] and superconductor/superconductor (S/S) [10,11] multilayers. A very useful theoretical study on the superlattice superconductor was given by Takahashi and Tachiki [12] based on their original formalism. At present, the anomalous behavior of $H_{C2\parallel}(T)$ is quite well-known and widely accepted as a fundamental property of superconductors with a layered structure.

* Corresponding author. E-mail: ikebe@iwate-u.ac.jp

0921-4534/99/$ - see front matter
PII: S0921-4534(99)00054-4

The anomalous behavior in temperature dependence, however, is not a monopoly of $H_{C2\parallel}(T)$ and the critical field perpendicular to the layer ($H_{C2\perp}$) also shows anomalous behavior. $H_{C2\perp}(T)$ of layer superconductors, quite often, does not follow the classical curves of Werthamer–Hefand–Hohenberg (WHH) [13] in pure and dirty limits but almost always deviates upward from the WHH curves.

In this paper, we present typical examples of anomalous $H_{C2\perp}$ of natural and artificial layer superconductors and discuss the origins which cause the anomalies. We will not discuss $H_{C2\perp}(T)$ of high-T_c oxides which also have layer structures, in which the upper critical field is hard explicitly to define and determine because of thermal activation of fluxoids. However, it is worthwhile to realize that the underlying $H_{C2\perp}$ of high-T_c oxides can appreciably deviate from the WHH curve from the analyses of $H_{C2\perp}$ of low-T_c layer superconductors.

2. Experimental

The alloy single crystals of the $Nb_{1-X}Ta_XSe_2$ and $Ta_{1-X}Nb_XS_2$ were grown by the iodine vapor transport method. The growth zone temperatures were set between 685 and 750°C. Pyridine (C_5H_5N) intercalation was carried out for $Ta_{1-X}Nb_XS_2$ by sealing the samples and pyridine in Pyrex ampoules with excess sulfur and reacting them at 200°C for about a week. Superlattice samples of Nb/Al_2O_3 (S/I) were fabricated by an rf sputtering method. The thickness of each sublayer (d_{Nb} and $d_{Al_2O_3}$) was designed over the range from 5 to 100 Å. The multilayer structures were confirmed by an X-ray diffraction. The superconducting transition temperature T_c and the upper critical field H_{C2} were resistively determined by a four terminal method. The magnetic field up to 100 kOe were applied by a superconducting magnet.

3. Crystal structures and physical properties of transition metal dichalcogenides

The layered structure of transition metal dichalcogenides consists of X–M–X unit sandwich sheets. The bonding within the sandwich is covalent and strong, while that between them is weak van der Waals type. Intercalated organic molecules take the sites between the unit layer of sandwich structure. There are two types of the sandwich layers with different electronic properties, which are characterized by the octahedral or trigonal prismatic coordination of chalcogen X around the transition metal M. The trigonal prismatic layers generally show metallic and superconductive properties, while octahedral layers show semiconductive behavior. The 2H polytype, which consists of only trigonal prismatic layers, show metallic conduction in both parallel and perpendicular directions. The 4Hb-polytype is of special interest because it consists of alternative accumulations of the trigonal prismatic (metallic) and the octahedral (semiconductive) layers. The electronic conduction of 4Hb-TaS_2, which is not superconductive above 1 K, was found to be metallic along the layer and semiconductive perpendicular to be layer probably as a result of the peculiar stacking of the two types layers. We found that the mixed crystal 4Hb-$Ta_{0.95}Nb_{0.05}S_2$ is superconductive with T_c = 2.92 K [14].

4. Results and discussion

4.1. Positive curvature anomaly in 4Hb polytype and pyridine intercalated $MX_2(Py)_{1/2}$

For an example of parallel and perpendicular critical field of MX_2 before and after the intercalation of organic molecules, Fig. 1 shows $H_{C2\parallel}$ and $H_{C2\perp}$ of 4Hb-$Ta_{0.95}Nb_{0.05}S_2$ and 4Hb-$Ta_{0.95}Nb_{0.05}S_2(Py)_{1/2}$. As a result of pyridine intercalation, $H_{C2\parallel}$ is greatly enhanced, while $H_{C2\perp}$ is significantly reduced. The enhancement of $H_{C2\parallel}$ accompanied with the reduction of $H_{C2\perp}$ is a common feature of the intercalation in all types of MX_2 compounds and, consequently, 2D character of superconductivity is enhanced. After the theory of Klemm, Ruther and Beakley (KLB) [5], the dimensionality of superconductivity is determined by a parameter γ which is defined by

$$\gamma = \frac{4}{\pi}\left[\frac{\xi_\perp(0)}{S/2}\right]^2, \qquad (1)$$

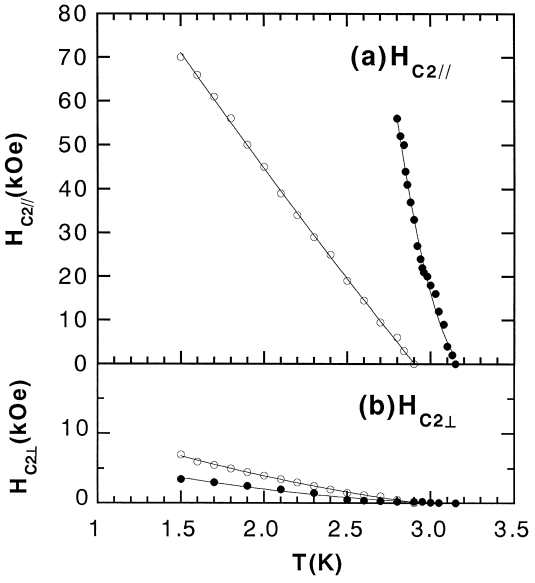

Fig. 1. $H_{C2\parallel}(T)$ and $H_{C2\perp}(T)$ of 4Hb-$Ta_{0.95}Nb_{0.05}S_2$ with (●) and without (○) pyridine intercalation.

where $\xi_\perp(0)$ is the zero temperature Ginzburg–Landau coherence length perpendicular to the layer and S is the distance between spacings of the M layer. S is nearly doubled (6 → 12 Å) by (Pyridine) intercalation and $\xi_\perp(0)$ is given by

$$\xi_\perp(0) = \xi_\parallel(0)\left[H_{C2\perp}/H_{C2\parallel}\right]_{T\approx T_c}, \qquad (2)$$

and the zero temperature parallel coherence length $\xi_\parallel(0)$ is determined by

$$T_c(-dH_{C2\perp}/dT)_{T\approx T_c} = \phi_0/2\pi\xi_\parallel^2(0), \qquad (3)$$

where ϕ_0 is the flux quantum. Estimated parameter values for the present samples of MX_2 are summarized in Table 1. For $\gamma < 1.76$, superconductivity becomes quasi-2D and the dimensional crossover takes place at T_D. At T_D, $H_{C2\parallel}$ limited by the orbital effect diverges and $H_{C2\parallel}$ of MX_2 is determined mainly by the Pauli-paramagnetism. In Fig. 1 we notice that $H_{C2\parallel}$ of 4Hb-$Ta_{0.95}Nb_{0.05}S_2(Py)_{1/2}$ behaves anomalously on temperature T, while $H_{C2\parallel}$ of 4Hb-$Ta_{0.95}Nb_{0.05}S_2$ shows linear dependence on T. But it must not be overlooked that $H_{C2\perp}$ of both intercalated and non-intercalated 4Hb-$Ta_{0.95}Nb_{0.05}S_2$ shows quite anomalous dependence on T. In order to see the anomalous behavior of $H_{C2\perp}$ of MX_2 more clearly, Fig. 2 presents the normalized critical field $h_{C2\perp} = H_{C2\perp}(t)/(-dH_{C2\perp}/dt)$ vs. the reduced temperature $t = T/T_c$ together with examples of 2H polytypes. In this figure, a distinct upward curvature is noticed for $h_{C2\perp}$ of intercalated compounds and non-intercalated 4Hb polytypes. We denote this type of anomaly as positive curvature anomaly (PCA). The $h_{C2\perp}$ curve of 2H-$Ta_{0.7}Nb_{0.3}S_2$ does not show clear PCA but it shows a minor anomaly, i.e., $h_{C2\perp}(T)$ follows almost T-linear dependence down to very low temperatures (linearity anomaly: LA), exceeding the WHH curves in low temperature regions.

First, we discuss the origin of PCA. Now it is widely recognized that the Anderson localization damages superconductivity mainly through the enhancement of the coulomb repulsion u^* between electrons and the depression of the electron density of state $N(0)$ [15]. Taking account of quantum corrections due to the Anderson localization, Maekawa, Ebisawa and Fukuyama (MEF) [16] calculated $H_{C2\perp}$ of dirty 2D systems and predicted the occurrence of the PCA anomaly. According to MEF, PCA is caused mainly by the enhanced coulomb repulsion u^* in the weak localization regime, which is weakened in the perpendicular magnetic field. Fig. 3 shows the temperature dependence of the electrical resistance of 2H-$Ta_{0.7}Nb_{0.3}S_2(Py)_{1/2}$ which was reacted for two weeks in an ampoule. The two-week reaction resulted in significant destruction of the sealed compounds and the resistance measurement was performed on a fragment of the obtained samples. In Fig. 3, the resistance minimum is discernible at about 15 K, which is consistent with the occurrence of the Anderson localization. Although PCA occurred for all the Py intercalation compounds, the resistance minimum was observed only in the fully intercalated fragments of partially destroyed compounds with small residual resistance ratio (RRR < 2). It seems that very slight imperfect intercalation quite easily masked out the resistance minimum. However, the existence of the resistance minimum supports the Anderson localization as the origin of PCA in $H_{C2\perp}$.

From the viewpoint of the Anderson localization as the origin of PCA, the behavior of $H_{C2\perp}$ and $H_{C2\parallel}$ of nonintercalated 4Hb-$Ta_{0.95}Nb_{0.05}S_2$ is worthwhile to reconsider. In Fig. 1, PCA is observable only in $H_{C2\perp}$ of 4Hb-$Ta_{0.95}Nb_{0.05}S_2$, which is

Table 1
Material parameters

	$Ta_{1-x}Nb_xS_2(Py)_{1/2}$			$Ta_{1-x}Nb_xS_2$			$Nb_{1-x}Ta_xSe_2$			Nb/Al_2O_3			
$d_{Nb}/d_{Al_2O_3}$										30/20	40/40	50/30	70/30
x	0.05	0.05	0.3	0.05	0.05	0.3	0.0	0.1	0.2				
Polytype	4Hb	2H	2H	4Hb	2H	2H	2H	2H	2H	–	–	–	–
$H_{C2\perp}$ anomaly[a]	PCA	PCA	PCA	PCA	LA	LA	LA	LA	LA	PCA	PCA	LA	–
T_C (K)	3.16	3.14	3.08	2.92	4.02	4.55	7.29	6.42	5.37	3.01	3.51	5.02	6.30
$(H_{C2\parallel}/H_{C2\perp})_{t\sim0.9}$	135	70	80	14	4.0	7.5	2.4	3.0	3.3	∞	∞	∞	∞
$(-dH_{C2\perp}/dT)_{t\sim0.9}$ (kOe/K)	1.35	1.65	1.50	3.30	7.30	5.55	7.5	8.3	8.0	5.0	5.3	5.6	4.4
$\xi_\perp(0)$ (Å)	2.1	3.4	3.2	13	25	16	33	21	23	–	–	–	–
γ	0.16	0.42	0.35	24	~100	37	>100	43	62	0	0	0	0
Dimension	q-2D	q-2D	q-2D	3D	3D	3D	3D	3D	3D	2D	2D	2D	2D
RRR	4.1	3.4	1.9	4.6	7.6	5.5	33	6.9	4.9	–	–	–	–

[a] See text.

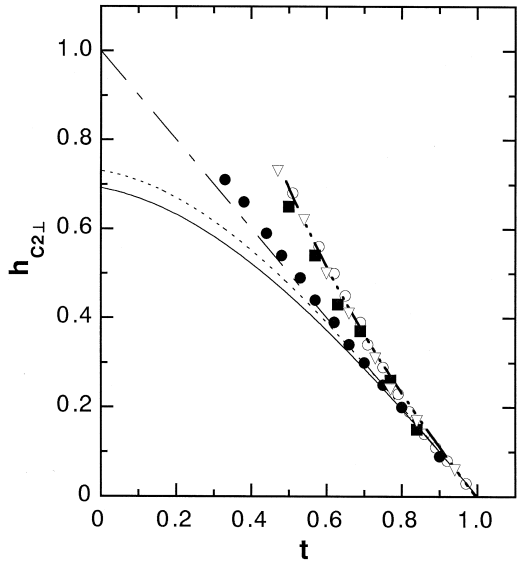

Fig. 2. The normalized perpendicular critical field $h_{C2\perp} = H_{C2\perp}(t)/(-dH_{C2\perp}/dt)_{t\sim0.95}$ vs. reduced temperature $t = T/T_c$ for sulfide compounds. ○: 4Hb-$Ta_{0.95}Nb_{0.05}S_2$, ▽: 4Hb-$Ta_{0.95}Nb_{0.05}S_2(Py)_{1/2}$, ●: 2H-$Ta_{0.7}Nb_{0.3}S_2$, ■: 2H-$Ta_{0.7}Nb_{0.3}S_2(Py)_{1/2}$. The solid and dotted curves are the WHH theoretical curves for the dirty and pure limit. The bold dash-dotted line (——– – – ———) is the calculation curves of Maekawa et al. [16] for $\lambda = 0.05$ and $\lambda_1 = 0.02$ (see text).

a 3D superconductor (see Table 1). $H_{C2\parallel}(T)$ of this compound follows T-linear relation in the measured temperature range and does not show any anomaly. This fact can be qualitatively understood on the basis of the Anderson localization. Under the magnetic field parallel to the layer, the electron orbital motion in the plane perpendicular to the field is subject to severe restriction because of the very large electric resistivity perpendicular to the layer plane. The delocalization effect due to the magnetic field which is the origin of PCA is far easy to occur in the $H_{C2\perp}$ geometry.

As we have mentioned in Section 3, 4Hb polytype contains similar octahedral layers as 1T-TaS_2 which consists of only octahedral layers. 1T polytype of TaS_2 is a typical material which shows the Anderson localization [17]. It is not unreasonable to assume that the octahedral layer is responsible for the Anderson localization also in 4Hb-$Ta_{0.95}Nb_{0.05}S_2$. The experimental data of the 3D superconductor, 4Hb-

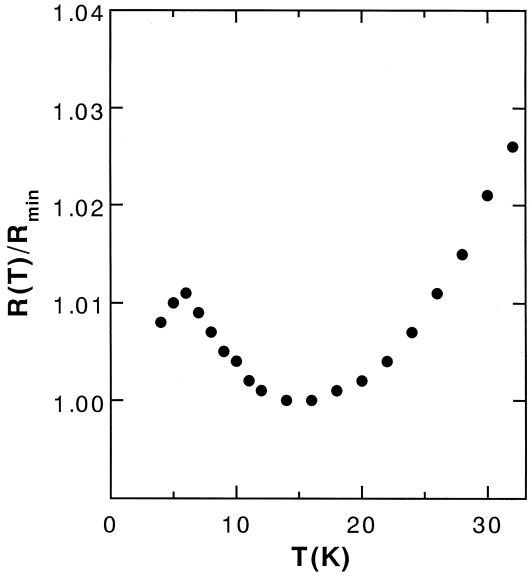

Fig. 3. The resistance minimum observed in 2H-$Ta_{0.7}Nb_{0.3}$-$S_2(Py)_{1/2}$. The temperature dependence of the resistance is consistent with the log T behavior for the case of the 2D weak Anderson localization between 6 K and 12 K.

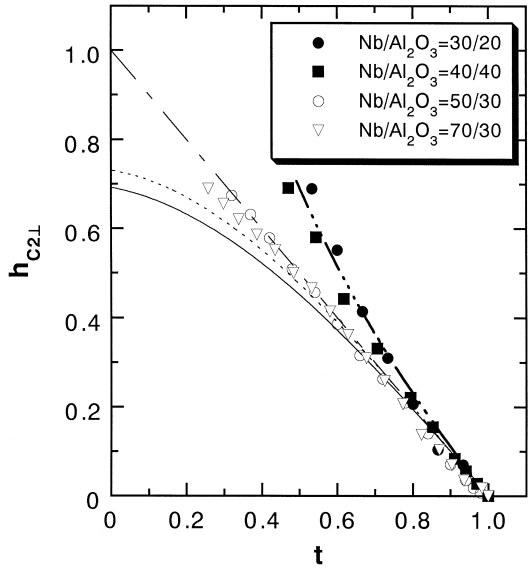

Fig. 4. $h_{C2\perp}$ vs. t for Nb/Al_2O_3 multilayers. A clear positive curvature is noticed for Nb layer thickness $d_{Nb} \leq 40$ Å. The bold dash-dotted line (——– – – ———) is the calculation curve of Maekawa et al. [16] ($\lambda = 0.05$, $\lambda_1 = 0.02$).

$Ta_{0.95}Nb_{0.05}S_2$, clarify that PCA is related to the orbital motion of electrons under magnetic fields and is not directly related to the dimensionality of superconductivity.

4.2. $H_{C2\perp}$ anomalies in Nb/Al_2O_3 superlattice

Anomalous behavior of $H_{C2\perp}$ is not peculiar only to naturally occurring layer compounds MX_2, but artificially prepared multilayer superconductors also show anomalous behaviors. In this subsection, we show and discuss $H_{C2\perp}$ anomalies of the superconductor/insulator multilayer Nb/Al_2O_3 [7,18]. Fig. 4 shows the renormalized perpendicular critical field $h_{C2\perp}$ vs. the reduced temperature t. With decreasing Nb layer thickness (d_{Nb}), the anomalous temperature dependence of $H_{C2\perp}$ is enhanced and $h_{C2\perp}$ of $d_{Nb} = 40$ Å and $d_{Nb} = 30$ Å shows PCA similar to $MX_2(Py)_{1/2}$. With increase of d_{Nb}, PCA disappears and linearity anomaly (LA) appears for $d_{Nb} = 50$ Å. Fig. 5 shows the sheet conductivity $G_\square$ per Nb sublayer as a function of d_{Nb}. $G_\square$ vs. d_{Nb}

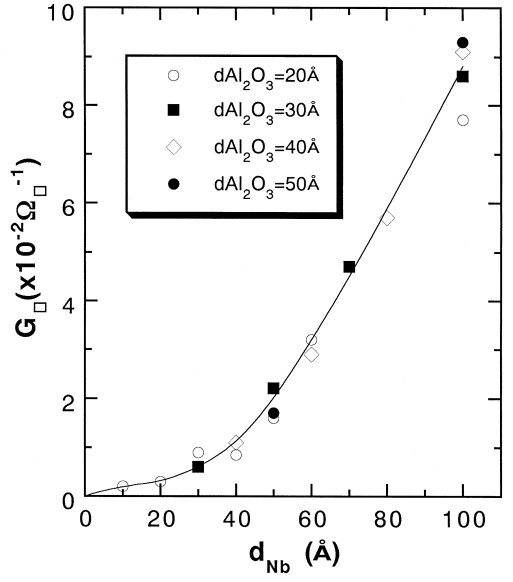

Fig. 5. The sheet conductance $G_\square$ vs. Nb layer thickness d_{Nb}. $G_\square$ shows an inflection point at around 40 Å and $G_\square$ is very small for $d_{Nb} \leq 40$ Å.

has a inflection point at around $d_{Nb} \sim 40$ Å and the sheet resistance $R_{\square}$ $(=1/G_{\square})$ is very large for $d_{Nb} \leq 40$ Å. This fact suggests that PCA of Nb/Al_2O_3, which occurs only for $d_{Nb} \leq 40$ Å, also originates from the Anderson localization. Here, it must be mentioned that PCA was observed only in the fully decoupled 2D Nb/Al_2O_3 samples with an infinite value of $(dH_{C2\parallel}/dT)_{T \approx T_c}$. For example, in Nb(40 Å)/Al_2O_3(20 Å) superlattice with quasi-2D superconductivity [7], $H_{C2\perp}$ showed only the linearity anomaly (LA).

4.3. Theoretical aspects of the Anderson localization and $H_{C2\perp}$

According to the theory and calculation due to Maekawa et al. [16], $H_{C2\perp}$ of 2D superconductors in the presence of the Anderson localization is determined by the following equations:

$$\ln\frac{T}{T_{c0}} = \psi\left(\frac{1}{2}\right) - \psi\left(\frac{1}{2} + \frac{eD_0H_{C2}}{2\pi T_c}\left(1 - \lambda\ln\frac{1}{T\tau_0}\right)\right) + R_{HF} + R_V, \quad (4)$$

$$R_{HF} = -\frac{\lambda_1}{2}\left(\ln\frac{1}{T\tau_0}\right)^2 - \lambda_1\left(\ln\frac{1}{T\tau_0}\right) \times\left[\psi\left(\frac{1}{2}\right) - \psi\left(\frac{1}{2} + \frac{eD_0H_{C2}}{2\pi T_c}\right)\right], \quad (5)$$

$$R_V = -\frac{\lambda_1}{3}\left(\ln\frac{1}{T\tau_0}\right)^3 - \lambda_1\left(\ln\frac{1}{T\tau_0}\right)^2 \times\left[\psi\left(\frac{1}{2}\right) - \psi\left(\frac{1}{2} + \frac{eD_0H_{C2}}{2\pi T_c}\right)\right]. \quad (6)$$

Here, R_{HF} and R_V are self-energy and vertex corrections of the Cooper pair propagator. $\psi(z)$ is the digamma function, τ_0 the electron relaxation time, D_0 the electron diffusion constant, and T_{C0} is the transition temperature in the absence of the Anderson localization. The two parameters λ and λ_1 are given by

$$\lambda = \frac{1}{2\pi\varepsilon_F\tau_0}, \quad (7)$$

where ε_F is the Fermi energy and

$$\lambda_1 = \frac{g_1N(0)}{2\pi\varepsilon_F\tau_0}, \quad (8)$$

where $N(0)$ is the electron density of state at ε_F and g_1 is the long ranged Coulomb interaction $(g_1 > 0)$. The T_c depression in the absence of the magnetic field is determined by the λ_1 value. In Figs. 2 and 4, the result of the calculation with $\lambda = 0.05$ and $\lambda_1 = 0.02$ is presented for comparison. The calculation curve reproduces the observed PCA quite well. However, the validity to use the parameter values, $\lambda = 0.05$ and $\lambda_1 = 0.02$ has not been established and must be examined carefully. Owing to complex distribution of the electrical current, to obtain unambiguous data on transport properties is usually very difficult in layered compounds and in superlattices.

4.4. On the origin of the linearity anomaly (LA)

Almost all nonintercalated MX_2 compounds [4] (except 4Hb-$Ta_{0.95}Nb_{0.05}S_2$ with PCA) and some of the Nb/Al_2O_3 multilayer samples [7] show linearity

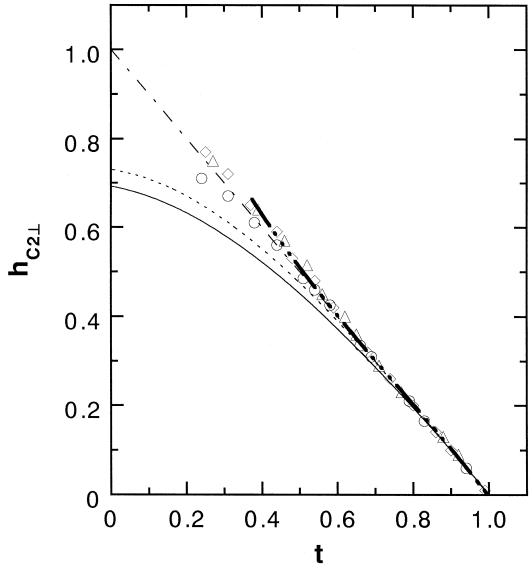

Fig. 6. $h_{C2\perp}$ vs. t for selenide compounds. ○: 2H-$NbSe_2$, ◇: 2H-$Nb_{0.9}Ta_{0.1}Se_2$, △: 2H-$Nb_{0.8}Ta_{0.2}Se_2$. The bold dash-dotted curve (——– – – ———) represents the calculation of Maekawa et al. [16] for $\lambda = 0.05$ and $\lambda_1 = 0.01$ (see text).

anomaly. Examples of LA of selenide 2H polytypes are shown in Fig. 6 and LA in 2H-$Ta_{0.7}Nb_{0.3}S_2$ and Nb(50 Å)/Al_2O_3(30 Å) can be seen in Figs. 2 and 4, respectively. According to the calculation of MEF, the $H_{C2\perp}(T)$ curve based on Eqs. (2), (4)–(6) reproduces LA if the parameter values $\lambda \sim 0.05$ and $\lambda_1 \sim 0.01$ are adopted. Thus LA in alloyed MX_2 compounds and Nb/Al_2O_3 multilayers, which are pretty dirty superconductors, can be naturally understood as also an effect of the weak Anderson localization in anisotropic 3D superconductivity regime. Then the main difference between PCA and LA comes from the difference in λ_1 value, i.e., strength of the Coulomb interaction $g_1N(0)$ in Eq. (8). For 2H-$Ta_{0.7}Nb_{0.3}S_2$, the depression of T_c caused by intercalation (4.55 → 3.08 K) is also consistent with the increase of λ_1(0.01 → 0.02). In Fig. 6, however, it must be noticed that 2H-$NbSe_2$ which is a pretty pure 3D superconductor [4] also shows LA. In case of 2H-$NbSe_2$, it seems more reasonable to ascribe LA to the anisotropies in the Fermi surface and the energy gap as a result of the nonlocal effect [19,20]. The origin of LA in layered superconductors is not unique and may depend on respective cases.

5. Summary

The anomalous behavior of the perpendicular critical field $H_{C2\perp}$ of natural and artificial superconductors with layered structure was analyzed mainly from the viewpoint of the weak Anderson localization. The conspicuous upward curvature (PCA) found in $Ta_{1-X}Nb_XS_2(Py)_{1/2}$ with quasi-2D superconductivity, 4Hb-$Ta_{0.95}Nb_{0.05}S_2$ with 3D superconductivity and Nb/Al_2O_3 multilayers ($d_{Nb} \leq 40$ Å) with 2D superconductivity is to come from the Anderson localization and is consistent with the theory due to Maekawa et al. [16]. The main origin of the less spectacular linearity anomaly (LA) found in nonintercalation alloy compounds, 2H-$Ta_{1-X}Nb_XS_2$ and 2H-$Nb_{1-X}Ta_XSe_2$ with anisotropic 3D superconductivity and LA in Nb/Al_2O_3 for $d_{Nb} \sim 50$ Å can also be understood as a remnant effect of the Anderson localization. But LA of 2H-$NbSe_2$, which is a pure anisotropic 3D superconductor, should be understood as to come from the anisotropies of the Fermi surface and the superconducting energy gap through the effect of nonlocality. The origin of LA which is very ubiquitous in layered superconductors is not unique and competition and interplay of several mechanisms must be taken into account.

Acknowledgements

One of the present authors (M.I.) wishes to thank Professor Maekawa and Professor Ebisawa for useful conversations.

References

[1] J.A. Wilson, F.J. Disalvo, S. Mahajan, Adv. Phys. 24 (1975) 117.
[2] D.E. Prober, R.E. Schwall, M.R. Beasley, Phys. Rev. B 21 (1980) 2717.
[3] R.C. Morris, R.V. Coleman, R. Bhandari, Phys. Rev. B 5 (1972) 895.
[4] M. Ikebe, Y. Muto, Synth. Met. 5 (1983) 229.
[5] R.A. Klemm, A. Luther, M.R. Beasley, Phys. Rev. B 12 (1975) 877.
[6] S.T. Ruggiero, T.W. Barbee, M.R. Beasley, Phys. Rev. B 26 (1982) 4894.
[7] M. Ikebe, Y. Obi, H. Fujishiro, H. Fujimori, J. Phys. Soc. Jpn. 62 (1993) 3680.
[8] C.S.L. Chun, G.G. Zheng, J.L. Vincent, I.K. Schuller, Phys. Rev. B 29 (1984) 4195.
[9] K. Kanoda, H. Mazaki, T. Yamada, N. Hosoito, T. Shinjo, Phys. Rev. B 33 (1986) 2052.
[10] Y. Obi, M. Ikebe, Y. Muto, H. Fujimori, Jpn. J. Appl. Phys. 26 (26 3) (1987) 1445, Suppl.
[11] M.G. Karkut, V. Matijasevic, L. Antognazza, J.M. Triscone, N. Missert, M.R. Beasley, F. Fisher, Phys. Rev. Lett. 60 (1988) 1751.
[12] S. Takahashi, M. Tachiki, Phys. Rev. B 33 (1986) 4620.
[13] N.R. Werthamer, E. Helfand, P.C. Hohenberg, Phys. Rev. 147 (1966) 295.
[14] M. Ikebe, K. Katagiri, Y. Muto, Physica B 108 (1981) 943.
[15] S. Maekawa, H. Fukuyama, J. Phys. Soc. Jpn. 51 (1983) 1352.
[16] S. Maekawa, H. Ebisawa, H. Fukuyama, J. Phys. Soc. Jpn. 52 (1983) 1352.
[17] N. Kobayashi, Y. Muto, Solid State Commun. 30 (1979) 337.
[18] Y. Kamiguchi, M. Ikebe, Y. Obi, H. Fujimori, Jpn. J. Appl. Phys. 30 (1991) 945.
[19] K. Takanaka, T. Nagashima, Prog. Theor. Phys. 43 (1970) 2890.
[20] D.W. Youngner, R.A. Klemm, Phys. Rev. B 21 (1980) 3890.